Non-Contrast Enhanced Renal MRA at 7T

Gregory J. Metzger[1], Ph.D. and Pierre-Francois van de Moortele[1], Ph.D.
[1]University of Minnesota, Center for Magnetic Resonance Research, Minneapolis MN

INTRODUCTION: Performing non-contrast enhanced renal angiography studies at 7T has the potential to improve the visualization of the first and second order branches as well as more distal arteries compared to lower field strengths and CE acquisitions (1). Along with the increased SNR expected at 7T, the higher T1s will result in longer inversion delays used for background suppression and thus better in-flow enhancement. Previous studies at lower fields have shown similar techniques to compete with contrast-enhanced studies at identifying significant renal artery stenosis (2,3) and for evaluating the vasculature post transplantation (4).

CHALLENGES: Many challenges must be overcome before the potential advantages of performing non-contrast enhanced renal angiography at 7T can be realized. First, with increasing field strength, inhomogeneities in the electromagnetic magnetic fields also increase. The spatial inhomogenetiy is a result of constructive and destructive interferences which occur as the size of the body is larger than the wavelength (~12 cm) at these frequencies (~ 300 MHz). While the spatially varying phase of the magnetic fields on receive (B1-) can be handled through magnitude reconstruction strategies such as sum-of-squares, no similar solution is available for transmit B1 (B1+) where the complex fields must be considered. By using multi-channel arrays driven by independent RF amplifiers, many different B1+ shimming strategies have been employed to optimize transmit fields in targeted regions in both head (5,6) and body (7,8) applications. The optimization strategy of choice depends on the target region's size, complexity, and location. In addition, the optimal solution may vary for individual RF pulses within an acquisition sequence. This was demonstrated by Hetherington et al. in the head (9), where different B1+ shim solutions optimizing homogeneity were used for performing outer volume suppression and spectroscopic localization. Similar strategies were employed in this study for achieving non-CE renal MRA however, unlike this previous work, the requirement of obtaining a rapid transmit B1 field estimation for B1+ shimming and the limited achievable peak B1+ realized at 7T in the body necessitated a different approach.

There is typically a tradeoff between the goals of obtaining B1+ efficiency and homogeneity. This tradeoff plays a critical role at 7T where current limitations in achievable peak B1+ in the body are a result of complex and destructively interfering RF fields, hardware limitations (RF coils, transmit chain efficiency, RF amplifier output) and local SAR constraints. If possible, it would be ideal to perform all imaging under a homogeneous transmit B1 distribution, but in many instances this is impractical at UHF. In order to achieve a uniform distribution over the renal arteries a tremendous price is paid in terms of RF efficiency greatly reducing the ability to suppress background signals.

METHODS: To address the challenges with transmit B1, subject dependent B1+ shimming was performed. Complex B1+ maps were estimated for each of the 16 channels using a fast, low flip angle, multi channel B1+ calibration scan (10). A multi-slice acquisition was able to acquire three slices in a single breath hold (11). The crucial point here is that the low flip angle approximation provides a relatively robust and rapid estimate of each transmit elements transmit profile which is required for the optimization routines employed. A contoured region of interested was selected on each of the three calibration scan slices to target B1+ optimization to the region of the renal arteries. Depending on the requirements for each RF pulse in the renal angiography sequence, different RF optimizations were implemented. The optimization routine allowed for solutions of RF efficiency or homogeneity. After each B1+ shim solution was applied, a quick (few seconds) small flip angle test image was obtained and compared against the pattern predicted by the B1 shim algorithm.

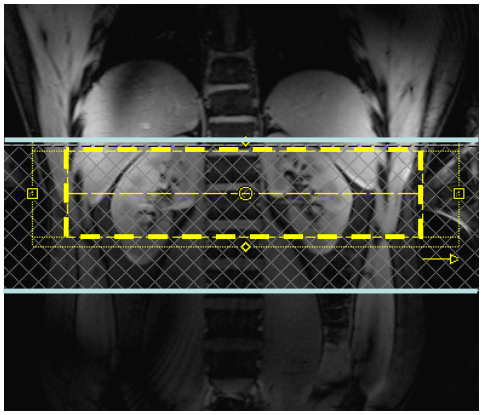

Figure 1: Planning of the angiography sequence. The excitation volume (yellow) and inversion volume (blue) are shown positioned on a coronal gradient echo image.

The basic non-CE acquisition strategy was a respiratory triggered turbo-flash (TFL) which consisted of a slab selective inversion and chemically shift selective fat suppression followed by a gradient-echo readout. Planning of the axial imaging and inversion volumes is shown in Fig. 1 following the strategy presented by Liu et al (4). The imaging parameters for the angiography sequence included the

following: 3.8 ms TR, 1.76 ms TE, 1000 ms TI, 8° nominal flip angle, GRAPPA = 2, 300 mm FOV, 72 slices with a nominal resolution of 1.0 to 1.2 mm isotropic. The requirements of homogeneity and peak B1+ vary tremendously between the adiabatic inversion and excitation pulses of the gradient echo readout, therefore RF pulse specific B1+ shim solutions were used. The inversion pulse was optimized using the transmit efficiency solution (Shim1) as it was more an issue of peak B1+, not homogeneity, which limited the quality of background suppression. To improve inversion performance even further, the standard adiabatic inversion pulse on the system, a 10 ms HS1, was modified to a 20-25 ms HS4 which requires a lower peak B1+ (12). For the excitation pulse, a second solution (Shim2) was employed which focused B1+ shimming on obtaining a homogeneous solution. Each B1+ shim solution consisted of a table of phases and gains which were loaded onto the amplifier's controller within ~5 μs. In order to accurately switch from one shim solution to the next, the acquisition sequence was programmed to send TTL triggers to the RF amplifier (Fig. 2), each of which initiated the loading of the appropriate table.

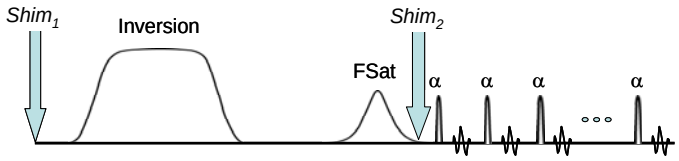

Figure 2: Angiography sequence with triggered B1+ shim solutions. *Shim*$_1$ → Efficiency, *Shim*$_2$ → Homogeneity.

The MRI system used in this studywas a 7T, 90cm bore magnet (Magnex, Oxford, UK) with a 32 channel console (Siemens Medical Solutions, Erlangen, Germany), using whole body gradients and 16 independent RF transceiver channels.

RESULTS: Figure 3 shows the results from a healthy subject. In Fig. 3 a, b and c, the middle of the three low flip angle test images are shown prior to any shimming (3a) and after the application of a B1+ shim optimizing for transmit efficiency (3b) and homogeneity (3c). The region used for B1+ optimization is shown by the broken curve in Fig. 3a and was individually drawn on the other two slices of the calibration scantowards the upper and lower poles. The signal intensity in these low flip angle calibration scans has consistently been an excellent predictor of B1+ shim efficiency and homogeneity. As expected the signal intensity in Fig. 3b shows the greatest B1+ in the kidneys but suffers from a local minimum across the right renal artery as shown by the yellow arrow and as demonstrated in the axial maximum intensity projection (MIP), Fig. 3d. While the homogenous solution, Fig. 3c, results in a loss in transmit efficiency, the local minimum present in the efficient solution is absent and enables the acquisition of the complete vasculature as demonstrated by the axial MIP in Fig. 3e. While the vessels are nicely visualized, the suppression of the background signal is incomplete which results from insufficient B1+ with the homogeneous solution.

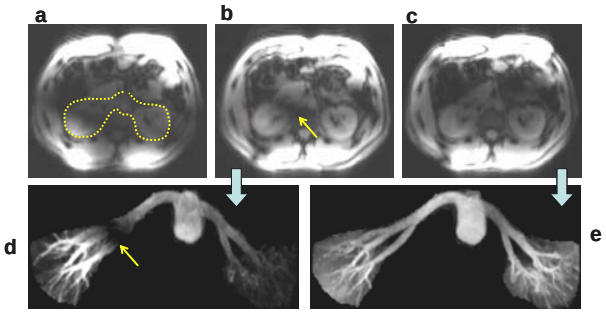

Figure 3: Low flip angle test images and cropped volumetric MIPs for the efficiency solution (b,d) and the homogeneous solution (c,e), respectively.

The triggered acquisition using efficiency for *Shim*$_1$ and homogeneity for *Shim*$_2$ are shown in Fig. 4 for two subjects.

DISCUSSION: We have found that the targeted homogeneous B1+ shimming solution based on the small flip calibration scans was necessary for consistently obtaining both branches of the renal arteries. In our hands, magnitude B1+ mapping in the large flip angle regime was a less robust approach with high sensitivity to physiological motion whatever technique was used, including AFI (13) and MP-TFL, therefore was not an option for optimizing B1+. Due to the robust and rapid nature of the single breath hold small flip angle calibration scan, it is directly suitable as-is for use in clinical studies.

Tailoring the optimization constraints to fit the

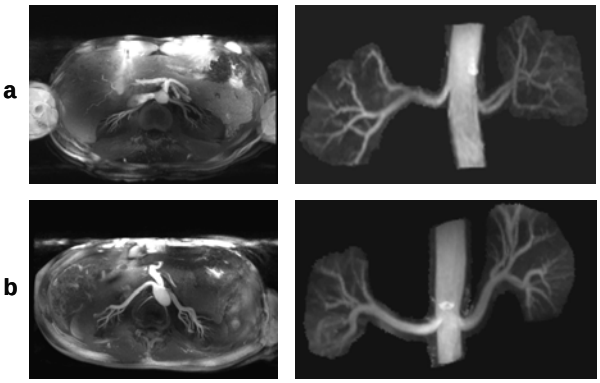

Figure 4: Angiography results from two individuals using efficiency for *Shim*$_1$ and homogeneity for *Shim*$_2$: (left) 40 mm MIPs, (right) cropped volumetric MIPs.

characteristics and function of each RF pulse was important. As shown in Fig. 3, the use of a single solution results in compromised image quality. As expected, the homogeneous solution is less efficient than the efficiency solution. This lack of efficiency results in two significant problems: 1) the power to reach the adiabatic condition for the inversion pulse is simply not realized and 2) even if enough power were available, the increased power deposition has the potential to exceed the local SAR limits. With the current hardware however, the practical issue is the inability to achieve the peak B1+ necessary for inversion. Due to the relatively short duty cycle of these respiratory triggered sequences, local SAR was not an issue in this study. Background suppression was reasonable when using the efficiency solution in most individuals. However, even with an adiabatic inversion pulse, local minima in B1+ resulted in incomplete inversion at some distal artery locations resulting in variable background suppression and venous contamination, Fig. 4b.

There are several possible ways to improve the quality and robustness of the presented methods. Higher transmit efficiency either from the perspective of the power train and/or the coil would increase the range of B1+ solutions which could be explored. On the algorithm front, shimming methods with constraints to guard against local minima could improve the consistency of background suppression when optimizing for efficiency. In addition, RF pulse design could play an equally important role as there are several methods available to obtain adiabatic inversion with lower peak B1+ requirements.

Once optimized, these methods will have to be compared against lower field strengths and other modalities to determine if the information obtained at 7T delivers on the potential of improved renal vasculature characterization.

ACKNOWLEDGEMENTS: Funding Provided by BTRC P41 - RR008079, and the Keck Foundation.

REFERENCES:

1. Wilson GJ, Maki JH. Non-contrast-enhanced MR imaging of renal artery stenosis at 1.5 tesla. Magn Reson Imaging Clin N Am 2009;17(1):13-27.
2. Maki JH, Wilson GJ, Eubank WB, Glickerman DJ, Pipavath S, Hoogeveen RM. Steady-state free precession MRA of the renal arteries: breath-hold and navigator-gated techniques vs. CE-MRA. J Magn Reson Imaging 2007;26(4):966-973.
3. Wyttenbach R, Braghetti A, Wyss M, Alerci M, Briner L, Santini P, Cozzi L, Di Valentino M, Katoh M, Marone C, Vock P, Gallino A. Renal artery assessment with nonenhanced steady-state free precession versus contrast-enhanced MR angiography. Radiology 2007;245(1):186-195.
4. Liu X, Berg N, Sheehan J, Bi X, Weale P, Jerecic R, Carr J. Renal transplant: nonenhanced renal MR angiography with magnetization-prepared steady-state free precession. Radiology 2009;251(2):535-542.
5. Adriany G, Van de Moortele PF, Ritter J, Moeller S, Auerbach EJ, Akgun C, Snyder CJ, Vaughan T, Ugurbil K. A geometrically adjustable 16-channel transmit/receive transmission line array for improved RF efficiency and parallel imaging performance at 7 Tesla. Magn Reson Med 2008;59(3):590-597.
6. Van de Moortele PF, Akgun C, Adriany G, Moeller S, Ritter J, Collins CM, Smith MB, Vaughan JT, Ugurbil K. B(1) destructive interferences and spatial phase patterns at 7 T with a head transceiver array coil. Magn Reson Med 2005;54(6):1503-1518.
7. Metzger GJ, Snyder C, Akgun C, Vaughan T, Ugurbil K, Van de Moortele PF. Local B1+ shimming for prostate imaging with transceiver arrays at 7T based on subject-dependent transmit phase measurements. Magn Reson Med 2008;59(2):396-409.
8. Snyder CJ, DelaBarre L, Metzger GJ, van de Moortele PF, Akgun C, Ugurbil K, Vaughan JT. Initial results of cardiac imaging at 7 Tesla. Magn Reson Med 2009;61(3):517-524.
9. Hetherington HP, Avdievich NI, Kuznetsov AM, Pan JW. RF shimming for spectroscopic localization in the human brain at 7 T. Magn Reson Med;63(1):9-19.
10. Van de moortelle P, Ugurbil K. Very fast multi-channel B1 calibration at high field in the small flip angle regime. In: Proceedings of the 17th Annual Meeting of ISMRM, Berlin, Germany 2009.
11. Metzger GJ, Simonson J, Bi X, Weale P, Zuehlsdorff S, Auerbach EJ, Ugurbil K, Van de Moortele PF. Initial Experiences with Non-Contrast Enhanced Renal Angiography at 7.0 Tesla. Proc Intl Soc Mag Reson Med 2010;18:#403.
12. Garwood M, DelaBarre L. The return of the frequency sweep: designing adiabatic pulses for contemporary NMR. J Magn Reson 2001;153(2):155-177.
13. Yarnykh VL. Actual flip-angle imaging in the pulsed steady state: a method for rapid three-dimensional mapping of the transmitted radiofrequency field. Magn Reson Med 2007;57(1):192-200.